Spin polarization and magnetic dichroism in photoemission from core and valence states in localized magnetic systems. IV. Core-hole polarization in resonant photoemission

Gerrit van der Laan
Daresbury Laboratory, Warrington WA4 4AD, United Kingdom

B. T. Thole
Material Science Center, University of Groningen, 9747 AG Groningen, The Netherlands
(Received 13 March 1995; revised manuscript received 24 August 1995)

A simple theory is presented for core-hole polarization probed by resonant photoemission in a two-steps approximation. After excitation from a core level to the valence shell, the core hole decays into two shallower core holes under emission of an electron. The nonspherical core hole and the final state selected cause a specific angle and spin distribution of the emitted electron. The experiment is characterized by the ground-state moments, the polarization of the light, and the spin and angular distribution of the emitted electron. The intensity is a sum over ground-state expectation values of tensor operators times the probability to create a polarized core hole using polarized light, times the probability for decay of such a core hole into the final state. We give general expressions for the angle- and spin-dependent intensities in various regimes of Coulomb and spin-orbit interaction: LS, LSJ, and jjJ coupling. The core-polarization analysis, which generalizes the use of sum rules in x-ray absorption spectroscopy where the integrated peak intensities give ground-state expectation values of the spin and orbital moment operators, makes it possible to measure different linear combinations of these operators. As an application the $2p_{3/2}3p3p$ decay in ferromagnetic nickel is calculated using Hartree-Fock values for the radial matrix elements and phase factors, and compared with experiment, the dichroism is smaller in the ^3P final state but stronger in the ^1D, ^1S peak.

I. INTRODUCTION

In papers I, II, and III,[1–3] we showed that the polarized photoemission from a core level is due to the alignment of the valence-band orbital and spin moments with the moments of the core hole created. The emission from an incompletely filled shell obeys the sum rules which relate the integrated intensities to the ground-state magnetic moments. Instead of photoemission we can also use x-ray-absorption spectroscopy (XAS), where sum rules give the orbital and spin magnetization, the spin-orbit operator $l \cdot s$ and the quadrupole moment of the ground state.[4] The core electron is excited into a polarized valence state and the dipole selection rules together with the Pauli principle result in a difference in absorption probability for left and right circularly polarized light. Thus XAS simply counts the number of core holes produced in the absorption irrespective of their kind. Apart from counting the emitted electrons we can also detect their direction, spin, and energy. Because each type of core hole emits electrons in different directions and with different spin polarization decaying to different final states we can obtain additional information about the core hole produced by the absorption step, which leads to improved knowledge of the original valence shell polarization.

Recently, Thole, Dürr, and van der Laan[5] reported a magnetic circular dichroism signal of 9% in the $2p3p3p$ decay of ferromagnetic nickel measured in a geometry where the circular dichroism in the $2p$ XAS is forbidden, i.e., with the helicity vector of the light perpendicular to the magnetization direction. The magnetic dichroism in the angle-integrated photoemission is then zero, however the magnetic dichroism in the photoemission along a noncollinear direction is not zero but provides a direct probe for the quadrupole moment of the core-hole state. This has the effect that with resonant photoemission we can measure combinations of the ground-state multipole moments other than those obtained from XAS.

Autoionization and related phenomena, such as two-photon excitation and Auger coincidence spectroscopy, have already been studied extensively in atomic physics[6] where the main aim was to perform "complete experiments" and to use known polarizations of the initial state in order to determine the radial matrix elements and phase shifts of the interfering decay channels.[7] As in the case of nonresonant photoemission in paper III, our approach for the solid state is the opposite. We assume that the radial matrix elements and phase factors for photoemission from deep core levels are known, e.g., from atomic Hartree-Fock calculations.[8] We use this complete knowledge of the decay process to study the polarization in the ground state caused by solid-state interactions, such as the molecular field (exchange interaction). We will decompose the core-core-core resonant photoemission intensity in such a way that it can be interpreted as a process in which first an excitation is made from a core level to a polarized valence shell, leaving behind a nonspherical core hole. After this the core hole decays to two shallower core holes in a specific state, which can be selected by the energy of the emitted photoelectron. The nonspherical nature of the core hole together with the properties of the selected final state then cause a specific spatial and spin distribution of the emitted electron. This approach neglects the destruction of interference[9,10] by electrostatic core-valence interactions, which will cause deviations from the simple behavior presented here. It is advantageous to study the decay from the

0163-1829/95/52(21)/15355(9)/$06.00

deep core-hole state into a shallower double core-hole state, because there is no direct photoemission and moreover the double core-hole state is highly localized having a well-defined wave function which simplifies the analysis. Decay processes involving open shells, such as core-core-valence and core-valence-valence decays, are more complicated and will not be discussed in this paper, neither will we treat photoelectron diffraction effects.[11] We will consider here excitation from core levels which have a large spin-orbit splitting. This gives the possibility to study spin properties by measuring angular distributions without spin detection.

The outline of this paper is as follows. The general theory is presented in Sec. II, where we also show under which conditions the process can be decomposed in an excitation and a decay step. For the three different types of coupling schemes, LS, LSJ, and jjJ, we will present expressions for the angle- and spin-dependent intensity as a sum over the ground-state tensor operators times the probability to create a core hole times the probability for decay of a core hole with specific moment. The angle dependence and symmetry properties of the experiment including spin detection are analyzed in Sec. III. As an application we calculate the measured Ni $2p3p3p$ decay spectrum in Sec. IV and conclusions are given in Sec. V. In the Appendix we derive general properties of angle-dependent functions, especially concerning parity.

II. THEORY

A. Decomposition in excitation and decay

We consider the resonant photoemission process $l^n \rightarrow \underline{c_j} l^{n+1} \rightarrow \underline{dp} l^{n+1} e$ consisting of a Q-pole absorption from a ground state $|g\rangle$ to a set of intermediate states $|i\rangle$ followed by the decay into final states $|f\rangle$ plus a continuum electron e. The state $|g\rangle$ has all core levels filled and the localized shell l only partly filled, such as the $3d$ level of transition-metal compounds or the $4f$ level of rare-earth materials. The c level has a large spin-orbit splitting and we consider transitions from the two levels $j=c\pm 1/2$ separately. The final states $|f\rangle$ have the deep core level filled and two holes in other, shallower core levels p and d, which have a large Coulomb interaction, and so the final states are split into well separated groups corresponding to different LS terms of the $\underline{pd}$ configuration. These terms are smeared out somewhat by the presence of the l shell but we will assume that this effect is small enough to consider the core-hole LS character as approximately pure. In heavier atoms the final-state core levels can also have large spin-orbit splitting and may be described more properly by LSJ coupling or even by $j_p j_d J$ coupling such as in the $2p3p3p$ decay of rare-earth ions.

The electric Q-pole transition matrix element T from the c_j level to the l level is given by

$$\sum_{\mathbf{1}\,\mathbf{2}} \langle i|l_{\mathbf{1}}^{\dagger} j_{\mathbf{2}}|g\rangle \langle l_{\mathbf{1}}|C_q^Q|j_{\mathbf{2}}\rangle \tag{1}$$

where we used **1**,**2**,... to denote the components $m_{1,2,\ldots}$ and $\sigma_{1,2,\ldots}$ of the momenta l,j, etc. Whether m, σ or both are meant is always clear from the context. To obtain elegant results we omit the radial integral and a coefficient n_{cQl} defined in Eq. (A8) of paper III. We keep the expansion in second quantization operators in order to preserve the full properties of the ground state, not specialized to a fixed coupling as is usual in atomic spectroscopy.

The decay matrix element due to Coulomb interaction V with a continuum level with symmetry e, with the electron measured in direction $\boldsymbol{\varepsilon}$ leaving behind the ion in state $|f\rangle$ is

$$\sum_{\mathbf{3}\,\mathbf{4}\,\mathbf{5}\,\mathbf{6}ke} \langle f|j_{\mathbf{3}}^{\dagger} d_{\mathbf{4}} p_{\mathbf{6}}|i\rangle Y_{m_5}^{e}(\boldsymbol{\varepsilon}) e^{i\delta_e} \langle e_{\mathbf{5}} j_{\mathbf{3}}|1/r_{12}|p_{\mathbf{6}} d_{\mathbf{4}}\rangle, \tag{2}$$

where δ_e is the phase shift of e, and the $Y_{m_5}^{e}$ is a spherical harmonic. The Coulomb matrix element is expanded in the radial integrals R_{cpde}^{k}. Equation (2) should also contain exchange terms with p and d interchanged. The behavior of these terms is exactly analogous in the derivation so that we will leave them out but include them in the end result.

B. Interference

For a two-core-hole final state there is no interference with direct photoemission, but there is still the interference effects between intermediate states. The general formula for the intensity is[9]

$$I(\omega,E_b)=\sum_{fii'} \frac{T_{gi'}V_{i'f}V_{fi}T_{ig}}{(E_{i'}-E_g-\omega+i\Gamma_{i'}/2)(E_i-E_g-\omega-i\Gamma_i/2)} \times \delta(E_f-E_g-E_b), \tag{3}$$

where $E_b=\omega-E_e$ is the binding energy, E_e is the energy of the emitted electron, i and f denote the intermediate and final states with energies E_i and E_f, respectively, T is the dipole operator and V is the Coulomb operator. First consider the intensity integrated at constant ω over an E_b range containing a set of states $\{f\}$ of interest, preferably well separated from the rest of the spectrum. Making the approximation that $E_i'=E_i$ one can integrate ω over a range containing a set of states $\{i\}$ well separated from other peaks and obtain

$$I_{\{f,i\}}=\sum_{\{f\}} I_{\{f\}}(\omega)d\omega=\sum_{\{ii'f'\}} \frac{2\pi}{\Gamma} T_{gi'}V_{i'f}V_{fi}T_{ig}, \tag{4}$$

which states the basic assumption precisely. Defining i to be a path from g to f when T_{gi} and V_{if} are both large, Eq. (4) is a good approximation if in the range $\{i\}$ there are no states i and i' forming a path from g to the same f and having energies differing by more than Γ.

The interference problem is absent in gas-phase experiments where atomic theory can be used, if we can find an intermediate LS or LSJ term which is well separated from rest of the spectrum, because the intermediate states are the degenerate $M_L M_S$ or M_J levels. Equation (4) is also exact in one-particle theory, where i denotes states with a core hole and with an extra valence electron in level ν_i. Then the levels i are not degenerate but $V_{if}V_{fi'}$ connects only states with the same energy because the ν level has no interaction with the core holes in i or f and so is a pure spectator in the decay: $\nu_i=\nu_{i'}$.

C. Removal of the core operators

Taking the square of the product of Eqs. (1) and (2) we obtain for the creation/annihilation part of the intensity

$$\sum_{ii'\,123461\underline{2}3\underline{4}\underline{6}} \langle g|j_{\underline{2}}^{\dagger} l_{\underline{1}}|i'\rangle\langle i'|p_{\underline{6}}^{\dagger} d_{\underline{4}}^{\dagger} j_{\underline{3}}|f\rangle\langle f|j_{\underline{3}}^{\dagger} d_4 p_6|i\rangle \times\langle i|l_{\underline{1}}^{\dagger} j_{\underline{2}}|g\rangle. \tag{5}$$

Here $|i\rangle$ denotes only states with a c_j hole but we can extend the summation over i to all states in the Hilbert space and use the closure relation because states without a c_j hole give only terms that are zero. We can now use

$$\langle f|j_3^{\dagger}\cdots j_2|g\rangle=\langle f|\cdots|g\rangle\delta_{23}, \tag{6}$$

and obtain

$$\langle g|l_{\underline{1}}p_{\underline{6}}^{\dagger}d_{\underline{4}}^{\dagger}|f\rangle\langle f|d_4p_6l_{\underline{1}}^{\dagger}|g\rangle\delta_{\underline{2}3}\delta_{\underline{2}\underline{3}}. \tag{7}$$

In this way the intensity is restricted to excitation and decay via the selected c_j states. The open l shell has been removed in the intermediate states by summing over all structure in the c_j edge caused by cl Coulomb interactions. So after having been inspected by the Pauli principle, the l shell is treated as a spectator in the rest of the process. In order to restrict the intensity to that of all final-state levels belonging to, e.g., a selected LS term of the $\underline{pd}$ configuration, irrespective of the state of the spectator $\underline{l}$ shell, we sum over all $|f\rangle$ which have pd hole in states belonging to this term. These $|f\rangle$ can be written as

$$|fLM_LSM_S\rangle\equiv\sum_{\underline{7}\,\underline{8}} d_{\underline{7}}p_{\underline{8}}|f_0\rangle\langle d_{\underline{7}}p_{\underline{8}}|LM\rangle\langle s\sigma_{\underline{7}}s\sigma_{\underline{8}}|SM_S\rangle, \tag{8}$$

where $|f_0\rangle$ runs over all states without any holes in p or d. The p and d hole states can be included into the summation after substitution into Eq. (7). Furthermore, because also $|g\rangle$ contains no core holes

$$\langle f_0|p_8^{\dagger}d_7^{\dagger}d_4p_6l_1|g\rangle=\delta_{68}\delta_{47}\langle f_0|l_1|g\rangle. \tag{9}$$

The summation over $|f_0\rangle$ gives a one-electron expectation value for $|g\rangle$ which can be expanded in expectation values of double tensor operators w^{xyz} as defined in Ref. 12, taking the place of the density matrix or statistical tensor in atomic theory. The summation over $246\underline{246}$ can now be performed using the δ factors. The expression for the intensity of the fundamental spectra for light polarized along $\mathbf{P}$ and spin polarization measured along $\mathbf{P_S}$ is obtained by multiplying the primitive spectra by $r^{sh}_{\sigma_5\sigma_{\underline{5}}}(\mathbf{P_S})$ and $r^{Qa}_{qq}(\mathbf{P})$, as defined in Eq. (5) of paper III, which are the coefficients required in the linear combinations of intensities.

D. Excitation step

To separate the excitation step from the decay step we introduce a summation over the moment r of the j core hole. The total expression for the angle- and spin-dependent emission intensity J_j^{ah} from the edge with total angular momentum j using polarized light of moment a and detecting the photoelectron spin of moment h for transition from a core state to the term LS of the two-core-hole state is

$$J_j^{ah}(LS;\mathbf{PP_S}\boldsymbol{\varepsilon}) =\frac{1}{4\pi}\sum_{zrb\zeta}\left\{\sum_{xy}\langle w_{\zeta}^{xyz}\rangle C_j^{xyzar}\right\}U_{\zeta}^{zarhb}(\mathbf{PP_S}\boldsymbol{\varepsilon})B_J^{rhb}(LS). \tag{10}$$

The interpretation is that given a ground state with moment xyz the dipole transition creates a core hole of moment r with probability C. The origin of this effect is the Pauli principle which allows the transition of the electron from the core into a valence level only if it is empty. Thus the absorption step probes the occupation of the valence levels and, depending also on the polarization of the light a it can create only specific core holes, resulting in a nonspherical core shell. The spin of the ground state ($y=1$) comes in through the spin-orbit coupling of the core level. The coefficient C is given by

$$C_j^{xyzar}(lcQ)=\sum_{\alpha}\begin{Bmatrix} j & r & j\\ s & y & s\\ c & \alpha & c\end{Bmatrix}\begin{Bmatrix} x & y & z\\ r & a & \alpha\end{Bmatrix}\begin{Bmatrix} c & \alpha & c\\ l & x & l\\ Q & a & Q\end{Bmatrix} \times[\alpha jclxyz]n_{lx}n_{sy}n_{xyz}n_{zar}n_{Qa}^{-1}n_{jr}^{-1}, \tag{11}$$

where the normalization coefficients n_{lx} are defined in paper III, Eq. (A7) and $[\alpha,...]$ is shorthand for $(2\alpha+1)\cdots$.

E. Decay step

1. LS coupling

The decay part of the intensity is given by the probability distribution for emission of an electron by the decay of the core hole with moment r into the LS states with two other core holes. The distribution is determined by the fact that one electron falls into the polarized core hole and together with the core electron which is emitted, it leaves behind the required LS level. The angular dependence is

$$U_{\zeta}^{zarhb}(\mathbf{PP_S}\boldsymbol{\varepsilon})=C_{\alpha}^{a}(\mathbf{P})C_{\gamma}^{h}(\mathbf{P_S})C_{\beta}^{b}(\boldsymbol{\varepsilon})\sum_{\alpha\rho\gamma\beta}\begin{pmatrix} z & a & r\\ \zeta & -\alpha & -\rho\end{pmatrix} \times\begin{pmatrix} r & h & b\\ \rho & -\gamma & -\beta\end{pmatrix}n_{zar}^{-1}n_{rhb}^{-1} \times(-)^{a-\alpha+r-\rho+h-\gamma+b-\beta}. \tag{12}$$

The coefficient B gives the probability that a core hole with moment r decays into the state LS and a photoelectron with orbital moment b and spin moment h

$$B_j^{rhb}(LS)=\begin{Bmatrix} c & b & c \\ s & h & s \\ j & r & j \end{Bmatrix}\begin{Bmatrix} s & h & s \\ s & S & s \end{Bmatrix}\sum_{e\underline{e}}\begin{Bmatrix} e & b & \underline{e} \\ c & L & c \end{Bmatrix}e^{i(\delta_e-\delta_{\underline{e}})}\sum_k\begin{Bmatrix} e & k & p \\ d & L & c \end{Bmatrix}R^k_{cpde}\sum_{\underline{k}}\begin{Bmatrix} p & \underline{k} & \underline{e} \\ c & L & d \end{Bmatrix}R^{\underline{k}}_{cpd\underline{e}}$$
$$\times(-)^{L+S}[LSjrcpde\underline{e}b]n_{jr}n_{ekp}n_{dkc}n_{c\underline{k}d}n_{pk\underline{e}}n_{eb\underline{e}}n_{sh}^{-1}\underline{n}_{bhr}. \tag{13}$$

Each summation of k in this expression is understood to contain also the term where p and d are interchanged together with a sign $(-)^{L+S}$. Because the $9j$ symbol has two equal columns $b+h+r$ must be even. The expression is symmetric under interchange of e and $\underline{e}$ and so $e^{i(\delta_e-\delta_{\underline{e}})}$ may be replaced by $\cos(\delta_e-\delta_{\underline{e}})$.

2. LSJ coupling

When one or both of the two final-state holes have appreciable spin-orbit coupling it may be possible to separate the different J levels of the LS term. The result is derived in the same way but for B we obtain

$$B_j^{rhb}(LSJ)=\sum_{e\underline{e}}\sum_{j_e j_{\underline{e}}}\begin{Bmatrix} L & c & e \\ S & s & s \\ J & j & j_e \end{Bmatrix}\begin{Bmatrix} e & b & \underline{e} \\ s & h & s \\ j_e & r & j_{\underline{e}} \end{Bmatrix}\begin{Bmatrix} \underline{e} & c & L \\ s & s & S \\ j_{\underline{e}} & j & J \end{Bmatrix}$$
$$\times\begin{Bmatrix} j & r & j \\ j_e & j & j_{\underline{e}} \end{Bmatrix}e^{i(\delta_e-\delta_{\underline{e}})}\sum_k\begin{Bmatrix} e & k & p \\ d & L & c \end{Bmatrix}R^k_{cpde}\sum_{\underline{k}}\begin{Bmatrix} p & \underline{k} & \underline{e} \\ c & L & d \end{Bmatrix}R^{\underline{k}}_{cpd\underline{e}}$$
$$\times(-)^{L+S}[LSJjrj_ej_{\underline{e}}cpd\underline{e}b]n_{jr}n_{ekp}n_{dkc}n_{c\underline{k}d}n_{pk\underline{e}}n_{eb\underline{e}}n_{sh}^{-1}\underline{n}_{bhr}. \tag{14}$$

Interchange of e,j_e and with $\underline{e},j_{\underline{e}}$ changes the product of the three $9j$ symbols by $(-)^{b+h+r}$. So for $b+h+r$ even we may replace the exponential by $\cos(\delta_e-\delta_{\underline{e}})$. For $b+h+r$ odd this is $-i\sin(\delta_e-\delta_{\underline{e}})$. The $-i$ is cancelled by the i in $\underline{n}_{bhr}$. This means that $b+h+r$ odd is allowed in LSJ coupling provided there are terms with $e\neq\underline{e}$ in the summation, in other words there is interference between the continuum channels e and $\underline{e}$.

3. jjJ coupling

When both final-state core holes have a spin-orbit coupling larger than their Coulomb interaction the observed final states may be described more appropriately as jjJ states, we obtain

$$B_j^{rhb}(j_pj_dJ)=\sum_{e\underline{e}}\sum_{j_ej_{\underline{e}}}\begin{Bmatrix} e & b & \underline{e} \\ s & h & s \\ j_e & r & j_{\underline{e}} \end{Bmatrix}\begin{Bmatrix} j & r & j \\ j_e & J & j_{\underline{e}} \end{Bmatrix}e^{i(\delta_e-\delta_{\underline{e}})}\sum_k R^k\begin{Bmatrix} e & k & p \\ j_p & s & j_e \end{Bmatrix}\begin{Bmatrix} d & k & c \\ j & s & j_d \end{Bmatrix}\begin{Bmatrix} j_p & k & j_e \\ j & J & j_d \end{Bmatrix}\sum_{\underline{k}}R^{\underline{k}}\begin{Bmatrix} \underline{e} & \underline{k} & p \\ j_p & s & j_{\underline{e}} \end{Bmatrix}$$
$$\times\begin{Bmatrix} d & \underline{k} & c \\ j & s & j_d \end{Bmatrix}\begin{Bmatrix} j_p & \underline{k} & j_{\underline{e}} \\ j & J & j_d \end{Bmatrix}(-)^{c+J+e+s+j_{\underline{e}}}[j_pj_dJjrj_ej_{\underline{e}}cpde\underline{e}b]n_{jr}n_{ekp}n_{dkc}n_{c\underline{k}d}n_{pk\underline{e}}n_{eb\underline{e}}n_{sh}^{-1}\underline{n}_{bhr}. \tag{15}$$

Interchange of e,j_e with $\underline{e},j_{\underline{e}}$ changes the $9j$ symbol together with the factor $(-)^{e+s+j_e}$ again by $(-)^{b+h+r}$ and so the same situation occurs as in LSJ coupling with respect to interference. In the summation over k there are again exchange terms where p and d are interchanged and the term is multiplied by $(-)^J$.

III. ANALYSIS

A. Excitation process

The important characteristics of the experiment are which type of moments, magnetic or nonmagnetic are being measured, whether linearly or circularly polarized light and/or spin detection are needed and which type of geometry is required. The coefficients C give the probability that a moment r is created in the core hole given the moments xyz in the ground state and using a polarized light. The value of r is in the range $0\cdots 2j$. The $9j$ symbols in Eq. (11) require that $x+a+\alpha$ and $r+y+\alpha$ both have to be even which means $x+y+a+r$ is even. We consider here only moments with even $x+y+z$ in the ground state, and so $z+a+r$ must be even. Odd (even) z means a (non) magnetic moment. Even a means isotropic ($a=0$) or linearly polarized light ($a=2$) and odd a means circular polarization ($a=1$). This determines the values of r induced in the core hole, especially whether they are even or odd. Each signal measures a linear combination of the $\langle w^{xyz}\rangle$ but these combinations depend on the values of z, a, and r.

The values of z, a, r, h, and b can be chosen by performing measurements in a number of geometries sufficient to determine all the coefficients of the angle dependence functions U^{zarhb} in Eq. (10) and selecting the combination desired. Assuming that the coefficients B are known, we can determine the linear combinations of $\langle w^{xyz}\rangle$ for a given z in Table I.

The sum rules for x-ray-absorption spectroscopy appear in these tables in the guise of sum rules for $r=0$. XAS measures the total number of core holes created, irrespective of their polarization, and this is exactly what $r=0$ (monopole) means. For $a=0$ we see from Table I that the sum of the C

TABLE I. The linear combinations of moments $\langle \underline{w}^{xyz} \rangle$ for p to d excitations with a polarized light and core-hole moment r. For even r the corresponding angle-dependent function is U^{zar0r} which implies spin-unpolarized measurement. For odd r spin-polarized measurement is necessary, with angle-dependent functions U^{zar1b} with $b=r-1$ and $b=r+1$. In the presence of spin-orbit coupling in the final state and interference between continuum channels, even r can also be studied by measurement of U^{zar1r}.

zar	$\sum_{xy} C^{xyzar}_{3/2} \underline{w}^{xyz}$	$\sum_{xy} C^{xyzar}_{1/2} \underline{w}^{xyz}$
000	$2\underline{w}^{000}+\underline{w}^{110}$	$\underline{w}^{000}-\underline{w}^{110}$
011	$\frac{1}{9}(5\underline{w}^{000}+4\underline{w}^{110})$	$\frac{1}{3}(\underline{w}^{000}-\underline{w}^{110})$
022	$\frac{1}{5}(\underline{w}^{000}+2\underline{w}^{110})$	
101	$\frac{1}{9}(10\underline{w}^{011}+15\underline{w}^{101}+2\underline{w}^{211})$	$\frac{1}{3}(-\underline{w}^{011}+3\underline{w}^{101}-2\underline{w}^{211})$
110	$\frac{1}{3}(\underline{w}^{011}+6\underline{w}^{101}+2\underline{w}^{211})$	$\frac{1}{3}(-\underline{w}^{011}+3\underline{w}^{101}-2\underline{w}^{211})$
112	$\frac{2}{15}(5\underline{w}^{011}+3\underline{w}^{101}+\underline{w}^{211})$	
121	$\frac{2}{45}(\underline{w}^{011}+15\underline{w}^{101}+11\underline{w}^{211})$	$\frac{2}{15}(-\underline{w}^{011}+3\underline{w}^{101}-2\underline{w}^{211})$
123	$\frac{3}{35}(7\underline{w}^{011}+2\underline{w}^{211})$	
202	$2\underline{w}^{112}+\underline{w}^{202}$	
211	$\frac{2}{45}(17\underline{w}^{112}+25\underline{w}^{202}+3\underline{w}^{312})$	$\frac{2}{15}(-2\underline{w}^{112}+5\underline{w}^{202}-3\underline{w}^{312})$
213	$\frac{3}{35}(14\underline{w}^{112}+\underline{w}^{312})$	
220	$\frac{1}{5}(2\underline{w}^{112}+10\underline{w}^{202}+3\underline{w}^{312})$	$\frac{1}{5}(-2\underline{w}^{112}+5\underline{w}^{202}-3\underline{w}^{312})$
222	$\frac{2}{35}(7\underline{w}^{112}+5\underline{w}^{202}+3\underline{w}^{312})$	

for $j=3/2$ and $j=1/2$ gives $3\langle \underline{w}^{000} \rangle = 3n_h$ and $C_{3/2}-2C_{1/2}=3\langle \underline{w}^{110} \rangle = -3\langle l \cdot s \rangle$. For $a=1$ we get $3\langle \underline{w}^{101} \rangle = (3/2)\langle L_z \rangle$ and $\langle \underline{w}^{011} \rangle + 2\langle \underline{w}^{211} \rangle = 2\langle S_z \rangle + 7\langle T_z \rangle$ and for $a=2$ we have $3\langle \underline{w}^{202} \rangle$ and $(6/5)\langle \underline{w}^{112} \rangle + (9/5)\langle \underline{w}^{312} \rangle$.

For $j=1/2$ it is clear that r can only be 0 and 1 and secondly that for each z the linear combination of w operators measured for fixed z but different a and r is the same, except for a constant factor.

B. Decay process

The second step in the process converts the core multipole into final states together with angular distributions and spin polarization of the emitted electron. If the final states are LS coupled states then $b+h+r$ is even, and because b is always even, $h+r$ has to be even. If the spin-orbit splitting in the final state is resolved and there is also interference between different continuum channels, the parity of $h+r$ is no longer restricted. Table II give an impression of the possibilities and is useful in working out applications.

C. Geometry and spin dependence

The angle-dependent function describes the behavior of the intensity when the directions of $\mathbf{P}$, $\mathbf{P_S}$, and $\boldsymbol{\varepsilon}$ are varied. We discuss here the properties of the functions U in cylindrical symmetry where the fact that $\langle w^{xyz}_{\zeta} \rangle$ must be totally symmetric simply means $\zeta=0$. In that case we may multiply U by $C^{z}_{\zeta}(\mathbf{M})$, which is $\delta_{\zeta 0}$ when $\mathbf{M}$ is along the Z axis, and by summing formally over ζ new functions $U^{zarhb}(\mathbf{MPP_S}\boldsymbol{\varepsilon})$ are obtained which are totally symmetric. These functions are described in the Appendix.

TABLE II. Allowed combinations of $zarhb$ for z up to 3 and r up to 2. Considering only $a+z+r$=even (no axially coupled tensors): if $r+h+b$=even and $h=0$ then $r=b$=even and $a+z$=even; if $r+h+b$=even and $h=1$ then r=odd and $a+z$=odd; if $r+h+b$=odd (spin-orbit coupling in final state and interference between continuum channels) then $h=1$ and $r=b$=even and $\neq 0$ and $a+z$=even. This table can be used together with Eq. (10) to find all terms in the summations for given a and h and z up to 3. The ultimate test for the presence of a term is a nonzero entry for zar in Table I for C, which automatically gives the corresponding values of x and y.

$r+h+b$	J^{ah}	$zarhb$				
Even	J^{00}	+++++	(00000)	(20202)		
	J^{01}	−+−−+	(10110)	(10112)		
	J^{10}	−−+++	(11000)	(11202)	(31202)	
	J^{11}	+−−−+	(01110)	(01112)	(21110)	(21112)
	J^{20}	+++++	(22000)	(02202)	(22202)	
	J^{21}	−+−−+	(12110)	(12112)	(32110)	(32112)
Odd	J^{01}	+++−+	(20212)			
	J^{11}	−−+−+	(11212)	(31212)		
	J^{21}	+++−+	(02212)	(22212)		

1. Spin-unresolved measurements

Without spin polarization the angular distributions involved are $U^{zab}(\mathbf{MP}\boldsymbol{\varepsilon})\equiv U^{zab0b}(\mathbf{MPP_S}\boldsymbol{\varepsilon})$. The U^{zab} are the same functions already defined[3] for off-resonance photoemission. For resonant photoemission, however, $z+a+b$ can only be even.

2. Spin polarization: Even functions

First we will consider the case that $r+h+b$ is even. Because b is even and $h=1$, r has to be odd and either $b=r-1$ or $b=r+1$. Because $z+a+r$ is even, $z+a+h+b$ is even. Therefore, according to rule 3 in the Appendix, U will be nonzero in general when all vectors are in the same plane. We will assume that in this case all relevant properties of U can be observed in coplanar geometries. The most important fact here is that when $\mathbf{M}$, $\mathbf{P}$, and $\boldsymbol{\varepsilon}$ are coplanar the polarization vector of $\mathbf{P_S}$ (defined formally in the Appendix) is also in the plane, because if $\mathbf{P_S}$ were perpendicular to it the signal would be zero because $z+a+b$ is odd (rule 1 in the Appendix). The overall pattern of geometries with transverse and radial polarization is determined by zar. Actually for the radial component of the polarization, which is measured when $\mathbf{P_S}$ is along $\boldsymbol{\varepsilon}$, we have generally, using Eq. (A2), $U^{zar1b}(\mathbf{MP}\boldsymbol{\varepsilon}\boldsymbol{\varepsilon})=U^{zar}(\mathbf{MP}\boldsymbol{\varepsilon})$, independent of b. So in resonant photoemission we have to measure distributions $U^{zar}(\mathbf{MP}\boldsymbol{\varepsilon})$ with even r to find the total intensity and with odd r to find the radial component of the spin polarization.

3. Spin polarization: Odd functions

The case when $r+h+b$ is odd is similar. Note that because b must be even, $b=r$ so that r is also even. Further, $\mathbf{P_S}$ is polarized perpendicularly to $\boldsymbol{\varepsilon}$ because the geometry $\mathbf{P_S}\|\boldsymbol{\varepsilon}$ is forbidden by rule 6 in the Appendix. It seems that again a geometry with $\mathbf{M}$, $\mathbf{P}$, and $\boldsymbol{\varepsilon}$ coplanar may be sufficient. In that case $\mathbf{P_S}$ is always perpendicular to the plane and the signal is thus automatically separated from signals with $b+h+r$ even. Again the distributions $U^{zar1r}(\mathbf{MPP_S}\boldsymbol{\varepsilon})$ and $U^{zar}(\mathbf{MP}\boldsymbol{\varepsilon})$ are strongly connected:

$$U^{zar1r}(\mathbf{MPP_S}\boldsymbol{\varepsilon})=(-)^{r+1}\frac{2}{2r+1}\frac{d}{d\varphi}U^{zar}(\mathbf{MP}\boldsymbol{\varepsilon}), \tag{16}$$

where φ denotes a rotation of $\boldsymbol{\varepsilon}$ around $\mathbf{P_S}$. So the derivative gives the change in intensity when $\boldsymbol{\varepsilon}$ is rotated around $\mathbf{P_S}$ keeping $\mathbf{M}$ and $\mathbf{P}$ fixed. Effectively this provides an alternative way to detect a given zar with even r.

IV. APPLICATION TO $2p3p3p$ DECAY

To illustrate the use of the theory we consider the decay of a $2p$ core hole into a double core-hole state in a $3d$ transition metal. The intensities J^{ah} for spin-integrated ($h=0$) and spin-polarized ($h=1$) photoemission using isotropic light ($a=0$) and circular ($a=1$) and linear ($a=2$) dichroism are obtained using Eq. (10), where the allowed combinations of $zarhb$ are given in Table II and $\Sigma_{xy}C_j^{xyzar}\underline{w}^{xyz}$ in Table I. The intensity $J^{10}_{1/2}$ has a $\mathbf{P}\cdot\mathbf{M}$ dependence exactly as the XAS signal, since for $r=0$ the core hole is not polarized. The results for the $j=3/2$ edge are more interesting

$$4\pi J^{00}_{3/2}=(2\underline{w}^{000}+\underline{w}^{110})U^{00000}B^{000}_{3/2}+(2\underline{w}^{112}+\underline{w}^{202})U^{20202}B^{202}_{3/2}, \tag{17}$$

$$4\pi J^{10}_{3/2}=\frac{1}{3}(\underline{w}^{011}+6\underline{w}^{101}+2\underline{w}^{211})U^{11000}B^{000}_{3/2}+\frac{2}{15}(5\underline{w}^{011}+3\underline{w}^{101}+\underline{w}^{211})U^{11202}B^{202}_{3/2}+\frac{3}{5}(2\underline{w}^{213}+\underline{w}^{303})U^{31202}B^{202}_{3/2}, \tag{18}$$

where the U functions in the circular dichroism are

$$U^{11000}=\mathbf{M}\cdot\mathbf{P}, \tag{19}$$

$$U^{11202}=-\frac{1}{2}\mathbf{M}\cdot\mathbf{P}+\frac{3}{2}(\mathbf{M}\cdot\boldsymbol{\varepsilon})(\boldsymbol{\varepsilon}\cdot\mathbf{P}), \tag{20}$$

$$U^{31202}=-\frac{1}{2}\mathbf{M}\cdot\mathbf{P}-(\mathbf{M}\cdot\boldsymbol{\varepsilon})(\boldsymbol{\varepsilon}\cdot\mathbf{P})+\frac{5}{2}(\mathbf{M}\cdot\mathbf{P})(\boldsymbol{\varepsilon}\cdot\mathbf{M})^2. \tag{21}$$

Thus by changing the angles between $\mathbf{P}$, $\boldsymbol{\varepsilon}$, and $\mathbf{M}$ we can separate the three different linear combinations of $\underline{w}^{xyz}$.

The B values for the $p_{3/2}pp$ decay are

$$B^{000}_{3/2}(^3P)=2B^{202}_{3/2}(^3P)=3\left(R^0_p-\frac{1}{5}R^2_p\right)^2, \tag{22}$$

$$B^{000}_{3/2}(^1S)=-B^{202}_{3/2}(^1S)=\frac{1}{3}\left(R^0_p+\frac{2}{5}R^2_p\right)^2, \tag{23}$$

$$B^{000}_{3/2}(^1D)=\frac{5}{3}\left(R^0_p+\frac{1}{25}R^2_p\right)^2+\frac{18}{125}(R^2_f)^2, \tag{24}$$

$$B^{202}_{3/2}(^1D)=-\frac{1}{6}\left(R^0_p+\frac{1}{25}R^2_p\right)^2-\frac{18}{25}R^2_f\left(R^0_p+\frac{1}{25}R^2_p\right)\cos(\delta_f-\delta_p)-\frac{36}{625}(R^2_f)^2. \tag{25}$$

Using for the Ni d^9 ppp decay the Hartree-Fock values[13] $R^0_p=0.07$ eV$^{1/2}$, $R^2_p=0.045$ eV$^{1/2}$, $R^2_f=0.08$ eV$^{1/2}$, $\delta_f-\delta_p=2.45$ radians, we obtain the B^{000} and B^{202} spectra given in Fig. 1, together with the spin-dependent spectra B^{110}, B^{112}, and B^{312} obtained in similar way.

Since the ^1S and ^3P state can only be reached for one continuum state, their ratios B^{202}/B^{000} are fixed numbers, independent of the value of the radial integrals. ^1D can be

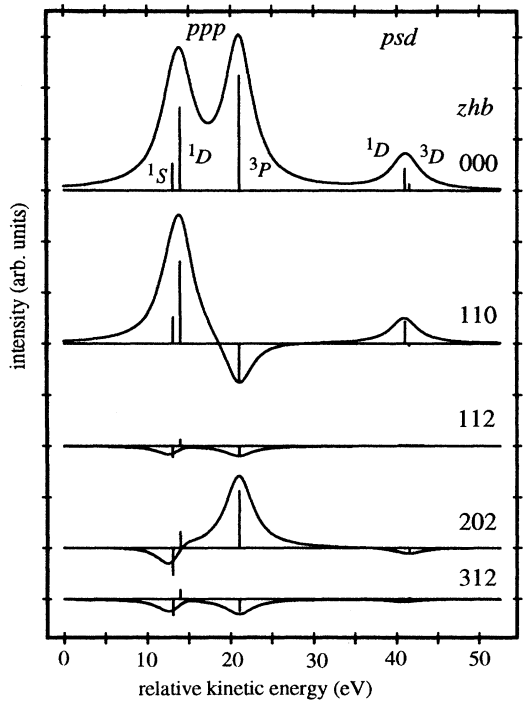

FIG. 1. Calculated $B^{zhb}_{3/2}$ spectra for ppp and psd decay in LS coupling for Ni d^9.

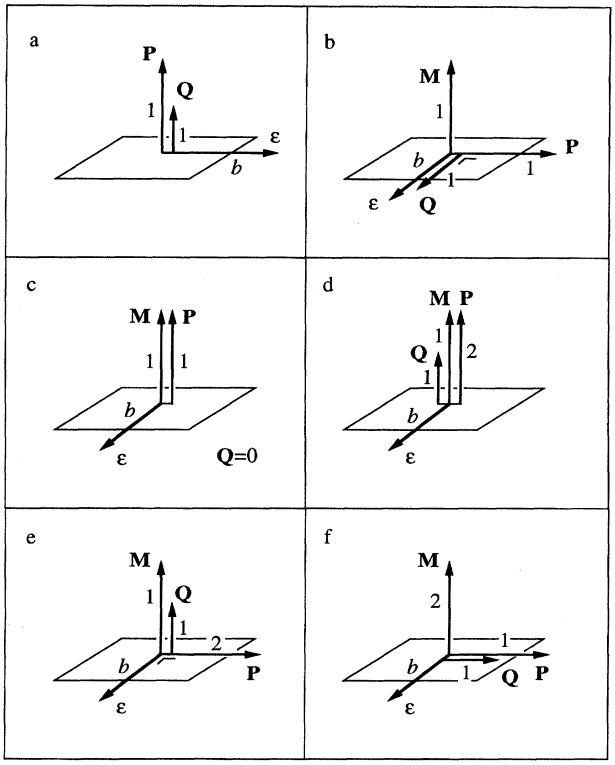

FIG. 2. Geometries in which the direction of $\mathbf{Q}$ (the polarization vector of $\mathbf{P_S}$) is fixed by the general properties of the angle-dependent functions. The intensity goes as $\mathbf{Q}\cdot\mathbf{P_S}$. The moments z and a of the magnetization $\mathbf{M}^{(z)}$ and the light polarization $\mathbf{P}^{(a)}$ are given in the pictures, for the photoemission direction ϵ the moment b is even. (a) $\mathbf{M}^{(0)}\rightarrow\mathbf{Q}\|\mathbf{P}^{(1)}$; (b) $\boldsymbol{\varepsilon}$ is $\|$ or $\perp\mathbf{M}^{(1)}$, $\mathbf{P}^{(1)}\rightarrow\mathbf{Q}\perp\mathbf{M},\mathbf{P}$; (c) $\mathbf{M}^{(1)}\|\mathbf{P}^{(1)}\perp\boldsymbol{\varepsilon}\rightarrow\mathbf{Q}=0$; (d) $\mathbf{M}^{(1)}\|\mathbf{P}^{(2)}\perp\boldsymbol{\varepsilon}\rightarrow\mathbf{Q}\|\mathbf{M}$; (e) $\mathbf{M}^{(1)}\perp\mathbf{P}^{(2)}\perp\boldsymbol{\varepsilon}\rightarrow\mathbf{Q}\|\mathbf{M}$; (f) $\mathbf{M}^{(2)}$ & $\mathbf{P}^{(1)}\rightarrow\mathbf{Q}\|\mathbf{P}$.

reached in the p and f channels and so the radial integrals and phase difference are important. Also to measure the spectra with odd $h+r$ requires interference between the channels.

The $3p^4$ final state in Fig. 1 has a strong intra-atomic configuration interaction (CI) with the $3s^1d^9$ final state (psd decay), which is split into a ^1D and ^3D state. The large CI matrix element pushes the ^1D peak of the $3s^1d^9$ structure toward the ^3D peak and the ^1D of the $3p^4$ structure toward the ^1S peak. This makes that the spectrum for the ppp decay is essentially split in a $^1S+{}^1D$ peak and a ^3P peak. Since the CI mixes the two ^1D states intensity is transferred between the two states and in the isotropic spectrum the $3s^1d^9$ gains intensity.

The isotropic spectrum B^{000} shows a triplet and a singlet peak with comparable intensities in agreement with experimental results and previous calculations.[13] The B^{110} spectrum gives the angle-integrated spin spectrum. Singlet states and triplet states have spin polarizations $(=B^{110}/B^{000})$ of 1 and $-1/3$, respectively. The spectra with $b\neq 0$ can only be observed in the angle dependence and they will vanish in the angle-integrated emission. In LS coupling the B^{312} spectrum is equal to the B^{112} spectrum times 3/2. Thus the angle dependence (i.e., $b=2$) is fully described by a spin-integrated spectrum B^{202} and a spin difference spectrum B^{112}.

Spin-orbit coupling in the final state splits the ^3P peak. This peak will display additional fine structure in the B^{110} and B^{202} spectra with opposite signs for the $^3P_2$ and $^3P_0$ levels. Spin-orbit coupling also introduces a difference between the B^{112} and B^{312} spectra. However, for the $3d$ metals the $3p$ spin-orbit coupling is small compared to the $3p$-$3p$ electrostatic interactions, so that the sum over the J levels, i.e., the LS coupling result, is a reasonable approximation.

In Ref. 5 the circular dichroism in the Ni ppp decay was measured for the geometry with $\mathbf{P}\cdot\mathbf{M}=0$, so that the B^{000} contribution vanishes. The J^{10} value is then proportional to $B^{202}_{3/2}$ which gives $^3P:(^1D+{}^1S)=1:(-0.12)$; CI changes this to $1:(-0.19)$. The experiment showed a smaller triplet peak but a larger singlet peak than the theory. In Ref. 5 this was accommodated by using the phase difference to fit the experiment. For $\delta_f-\delta_p=1.1$ radians $B^{202}_{3/2}(^1D)$ changes from 19.53 to -18.8, so that the J^{10} signal of $^1D+{}^1S$ gives about the same value as the ^3P signal with opposite sign. There is no obvious reason to assume that the Hartree-Fock value is so much in error because atomic calculations with different numbers of electrons, or even different core holes, do not change the value of the phase difference by more than a few hundredths.[14] It is of course possible that some of the signal is affected by satellite structure, photoelectron diffraction or Auger decay.

The angular dependence of the dichroism in Eq. (18) produces different linear combinations of the moment operatiors. For instance, the ratio w^{011} to w^{211} is ten times larger for the $z=2$ than for the $z=0$ term. This makes it possible, by

using the geometry $\mathbf{P}\perp\mathbf{M}$, to obtain the spin magnetic moment without a large correction from the magnetic dipole term, which is present in XAS.[5]

V. CONCLUSIONS

We considered the resonant photoemission intensity as an excitation from a core level to the valence shell, leaving behind a polarized core hole. After this the core hole decays into two shallower core holes in a specific state, which can be selected by the energy of the emitted photoelectron. The nonspherical nature of the core hole together with the properties of the selected final state cause a specific spatial and spin distribution of the emitted electron. The basic assumption underlying this type of analysis is that core-valence interactions do not destroy interference between intermediate states which are in the same edge by separating them by more than their lifetime width. This is correct in single-particle theory. Therefore, deviations from our results may be useful in the study of the validity of single-particle theory in the presence of core-valence interactions.

Measurement of the spin polarization appears to be useful to find the ground-state expectation values of all possible one-electron operators, even though spin-orbit coupling in the initial core hole already allows determination of spin properties from the angle dependence of spin-integrated experiments. The core-polarization analysis resembles the use of sum rules in x-ray-absorption spectroscopy, in that only an overall feature of the spectrum is used, while the whole two-dimensional spectrum contains much more information, especially due to the splitting caused by core-valence interactions.

APPENDIX: GENERAL PROPERTIES OF ANGLE-DEPENDENT FUNCTIONS

Consider the angle-dependent function U constructed from spherical harmonics coupled to a totally symmetric spherical function:

$$U^{zarhb}(\mathbf{MPP_S}\varepsilon)=C^z_\zeta(\mathbf{M})C^a_\alpha(\mathbf{P})C^h_\gamma(\mathbf{P_S})C^b_\beta(\varepsilon)\sum_{\zeta\alpha\rho\gamma\beta}\begin{pmatrix} z & a & r\\ -\zeta & -\alpha & -\rho\end{pmatrix}\begin{pmatrix} r & h & b\\ \rho & -\gamma & -\beta\end{pmatrix}$$
$$\times n_{zar}^{-1}n_{rhb}^{-1}(-)^{z-\zeta+a-\alpha+r-\rho+h-\gamma+b-\beta}. \tag{A1}$$

Upon inversion of a single vector $\mathbf{P}$ with associated moment l we obtain $C^l_m(-\mathbf{P})=(-)^lC^l_m(\mathbf{P})$ and so the whole function U changes by a sign $(-)^l$.

Rule 1. *General theorem:* a totally symmetric spherical function U of a set of vectors with associated moments is zero, if a part of these vectors is perpendicular to the plane containing all the other vectors, the sum of which moments is odd.

This can be shown by inverting all the vectors in the plane. Each inversion of a vector with moment l gives a factor $(-)^l$. The function U will thus change sign if the sum of the inverted moments is odd. But this geometry can also be obtained by a rotation of 180° around the axis perpendicular to the plane and so U in this geometry must have the same value as before rotation. Thus U must be zero.

We have the following special cases:

Rule 2. *All vectors collinear:* we may consider the collinear vectors to lie in a plane with zero vectors perpendicular to it. Then U is zero if the sum of the moments is odd.

Rule 3. *All vectors coplanar:* the sum of the moments of the vectors must be even.

Rule 4. *Two sets of collinear vectors perpendicular to each other:* both sets must be even.

Rule 5. *Three mutually perpendicular sets:* all three sets must be even or all must be odd.

Vectors with zero moment can be disregarded, but vectors with moment 1 are often special. If a totally symmetric function contains a vector with moment 1 it can be written as a normal inner product of two vectors. For example, a function of four vectors $\mathbf{P_a}$, $\mathbf{P_b}$, $\mathbf{P_d}$, and $\mathbf{P}$ with moments a, b, d, and 1, respectively, can be written as $\mathbf{P}\cdot\mathbf{Q}$ where $\mathbf{Q}$ is a function of $\mathbf{P_a}$, $\mathbf{P_b}$, and $\mathbf{P_d}$.

We may call $\mathbf{Q}$ the polarization vector of $\mathbf{P}$. Given the value of $\mathbf{Q}$ we know the whole angle dependence of the function on $\mathbf{P}$, being $U=\mathbf{P}\cdot\mathbf{Q}$, a simple cosine dependence. Now suppose that for some choice of values for the vectors the function is zero. Then the polarization vector of $\mathbf{P}$ must be perpendicular to $\mathbf{P}$ (or be zero). This information may help to fix $\mathbf{Q}$ completely and then we have the total dependence on $\mathbf{P}$. Figure 2 gives some examples of geometries with special consequences for the spin-polarization vector.

Special case: given a vector $\mathbf{P}$ of moment 1 and two even sets of collinear vectors, set_1 and set_2, perpendicular to each other the function is zero for all directions of $\mathbf{P}$.

This occurs, e.g., in Fig. 2(c). Proof: consider the case that $\mathbf{P}$ is in the plane of set_1 and set_2. U is then zero because the total sum is odd. So $\mathbf{Q}$ must be perpendicular to the plane. On the other hand, if $\mathbf{P}$ is perpendicular to the plane, set_1 is perpendicular to the plane of $\mathbf{P}$ and set_2, which are together odd and U is again zero. So $\mathbf{Q}$ must be in the plane. This is only possible if $\mathbf{Q}=0$ and so the whole function is zero for any $\mathbf{P}$ (keeping the other vectors constant). Note that if the moment of $\mathbf{P}$ is not 1 but, e.g., 3 then U is again zero for $\mathbf{P}$ either in the plane or perpendicular to it, but not necessarily in any other direction.

There is one important extra rule which also includes "internal moments."

Rule 6. *Collinear reduction:* When two vectors $\mathbf{P_a}$ and $\mathbf{P_b}$ with moments a and b are coupled to c the expression is zero when $\mathbf{P_a}$ and $\mathbf{P_b}$ are parallel and $a+b+c$ is odd.

This is due to the relation

$$C^a_\alpha(\mathbf{P_a})C^b_\beta(\mathbf{P_b})(-)^{a-\alpha+b-\beta}\begin{pmatrix} a & b & c \\ -\alpha & -\beta & \gamma \end{pmatrix} = C^c_\gamma(\mathbf{P_c})\begin{pmatrix} a & b & c \\ 0 & 0 & 0 \end{pmatrix}, \tag{A2}$$

where the last $3j$ symbol is zero for $a+b+c$ odd.

[1] B. T. Thole and G. van der Laan, Phys. Rev. B **44**, 12 424 (1991).

[2] G. van der Laan and B. T. Thole, Phys. Rev. B **48**, 210 (1993).

[3] B. T. Thole and G. van der Laan, Phys. Rev. B **49**, 9613 (1994).

[4] G. van der Laan and B. T. Thole, Phys. Rev. Lett. **60**, 1977 (1988); B. T. Thole and G. van der Laan, Phys. Rev. A **38**, 1943 (1988); B. T. Thole, P. Carra, F. Sette, and G. van der Laan, Phys. Rev. Lett. **68**, 1943 (1992); P. Carra, B. T. Thole, M. Altarelli, and X. Wang, *ibid.* **70**, 694 (1993); P. Carra, H. König, B. T. Thole, and M. Altarelli, Physica B **192**, 182 (1993); G. van der Laan, J. Phys. Soc. Jpn. **63**, 2393 (1994).

[5] B. T. Thole, H. A. Dürr, and G. van der Laan, Phys. Rev. Lett. **74**, 2371 (1995).

[6] S. Flügge, W. Mehlhorn, and V. Schmidt, Phys. Rev. Lett. **29**, 7 (1972); B. Cleff and W. Mehlhorn, J. Phys. B **7**, 593 (1974); **7**, 605 (1974); S. C. McFarlane, *ibid.* **5**, 1906 (1972); N. M. Kabachnik and I. P. Sazhina, *ibid.* **9**, 1681 (1976); E. G. Berezhko, N. M. Kabachnik, and V. S. Rostovsky, *ibid.* **11**, 1749 (1977); K. Blum, B. Lohmann, and E. Taute, *ibid.* **19**, 3815 (1986); N. M. Kabachnik and O. V. Lee, *ibid.* **22**, 2705 (1989); B. Lohmann, *ibid.* **23**, 3147 (1990); **24**, 861 (1991); J. Berakdar, H. Klar, A. Huetz, and P. Selles, *ibid.* **26**, 1463 (1993); B. Lohmann, U. Hergenhahn, and N. M. Kabachnik, *ibid.* **26**, 3327 (1993); B. Lohmann and F. P. Larkins, *ibid.* **27**, L143 (1994).

[7] H. Klar, J. Phys. B **13**, 4741 (1980).

[8] R. D. Cowan, *The Theory of Atomic Structure and Spectra* (University of California Press, Berkeley, 1981).

[9] J. J. Sakurai, *Advanced Quantum Mechanics* (Addison-Wesley, New York, 1967), Chap. 2.6.

[10] J. Aberg and G. Howat, in *Handbuch der Physik*, edited by W. Mehlhorn (Springer, Berlin, 1982), Vol. 31, p. 469; C.-O. Almbladh and L. Hedin, in *Handbook on Synchrotron Radiation*, edited by E.-E. Koch (North-Holland, Amsterdam, 1983), Vol. 1b, Chap. 8.

[11] J. J. Rehr and R. C. Alberts, Phys. Rev. B **41**, 8139 (1990); Y. U. Idzerda and D. E. Ramaker, Phys. Rev. Lett. **69**, 1943 (1992); D. E. Ramaker, H. Yang, and Y. U. Idzerda, J. Electron Spectrosc. Relat. Phenom. **68**, 63 (1994).

[12] B. T. Thole, G. van der Laan, and M. Fabrizio, Phys. Rev. B **50**, 11 466 (1994), Eqs. (14) and (17).

[13] G. van der Laan, M. Surman, M. A. Hoyland, C. F. J. Flipse, B. T. Thole, Y. Seino, H. Ogasawara, and A. Kotani, Phys. Rev. B **46**, 9336 (1992).

[14] S. M. Goldberg, C. S. Fadley, and S. Kono, J. Electron Spectrosc. Relat. Phenom. **21**, 285 (1981).